Threshold Region Performance Prediction for Adaptive Matched Field Processing Localization

Nigel Lee and Christ D. Richmond
MIT Lincoln Laboratory
244 Wood Street
Lexington, MA 02420-9108
phone: 781-981-2908
email: nigel@ll.mit.edu
email: christ@ll.mit.edu

Abstract Matched field processing (MFP) provides a means of attaining the full gains available from the shallow-water acoustic channel in passive sonar signal processing. By modeling the full field structure of acoustic signals propagating in the ocean, MFP offers the potential for both detection gain (through its better signal model) and localization gain (through its additional discrimination capability in range and depth) over traditional planewave processing. However, high spatial ambiguities and mismatch present formidable challenges in practice, limiting the performance gains that are realistically achievable with MFP.

Prediction of MFP localization performance is a challenging problem. MFP replica (steering) vectors can be highly ambiguous in range and depth, resulting in significant non-local estimation errors at low signal-to-noise ratios (SNRs)—errors not modeled by traditional localization measures such as the Cramer-Rao bound. Recent work has demonstrated the accuracy of an interval-error-based method, referred to herein as the "method of interval errors" (MIE), in predicting mean-squared error localization performance well into the threshold region where non-local errors may dominate.

This work uses the MIE to predict the mean-squared error accuracy of MFP range and depth estimates for two well-known approaches: (i) conventional beamforming (equivalent to maximum likelihood estimation for white noise) and (ii) Capon-MVDR adaptive beamforming. Simulation results will characterize localization performance as a function of SNR, for apertures and environments of interest. Particular attention will be given to the "threshold SNR" (below which localization performance degrades rapidly due to global estimation errors) and to the minimum SNR required to achieve acceptable range/depth localization. Initial work will also be presented assessing the MIE's potential to characterize localization performance in the presence of mismatch.

Report Documentation Page

Form Approved
OMB No. 0704-0188

1. REPORT DATE	2. REPORT TYPE	3. DATES COVERED
20 DEC 2004	**N/A**	**-**

4. TITLE AND SUBTITLE	5a. CONTRACT NUMBER
Threshold Region Performance Prediction for Adaptive Matched Field Processing Localization	5b. GRANT NUMBER
	5c. PROGRAM ELEMENT NUMBER
6. AUTHOR(S)	5d. PROJECT NUMBER
	5e. TASK NUMBER
	5f. WORK UNIT NUMBER
7. PERFORMING ORGANIZATION NAME(S) AND ADDRESS(ES) **MIT Lincoln Laboratory 244 Wood Street Lexington, MA 02420-9108**	8. PERFORMING ORGANIZATION REPORT NUMBER
9. SPONSORING/MONITORING AGENCY NAME(S) AND ADDRESS(ES)	10. SPONSOR/MONITOR'S ACRONYM(S)
	11. SPONSOR/MONITOR'S REPORT NUMBER(S)

12. DISTRIBUTION/AVAILABILITY STATEMENT
Approved for public release, distribution unlimited

13. SUPPLEMENTARY NOTES
See also, ADM001741 Proceedings of the Twelfth Annual Adaptive Sensor Array Processing Workshop, 16-18 March 2004 (ASAP-12, Volume 1)., The original document contains color images.

14. ABSTRACT

15. SUBJECT TERMS

16. SECURITY CLASSIFICATION OF:			17. LIMITATION OF ABSTRACT	18. NUMBER OF PAGES	19a. NAME OF RESPONSIBLE PERSON
a. REPORT	b. ABSTRACT	c. THIS PAGE			
unclassified	**unclassified**	**unclassified**	**UU**	**10**	

THRESHOLD REGION PERFORMANCE PREDICTION FOR ADAPTIVE MATCHED FIELD PROCESSING LOCALIZATION

Nigel Lee, Christ D. Richmond

MIT Lincoln Laboratory
Advanced Sensor Techniques Group
nigel@ll.mit.edu, christ@ll.mit.edu

ABSTRACT

The full-field modeling of matched field processing (MFP) provides potentially large gains over traditional beamformers in passive sonar signal processing. MFP localization gains are manifested by superior estimation of source range and novel estimation of source depth. However, MFP localization is limited in practice by high spatial ambiguities in the MFP output. These ambiguities can result in *global* localization errors at low signal-to-noise ratios, errors which must be accounted for to predict MFP localization performance accurately. This work uses the so-called *method of interval errors* (MIE) to predict MFP mean-squared error localization performance well into the "threshold region" where global errors dominate. New results enable highly accurate threshold region MIE predictions for both conventional beamforming and Capon-MVDR adaptive beamforming in the simple signal-in-white-noise case. A variation of the standard MIE technique is shown to produce equally accurate performance predictions when both mismatch and colored noise are introduced.

1. INTRODUCTION

Matched field processing (MFP) provides a means of attaining the full gains available from the shallow-water acoustic channel in passive sonar signal processing. By modeling the full field structure of acoustic signals propagating in the ocean, MFP offers the potential for both detection gain (through its better signal model) and localization gain (through its superior estimation of source range and novel estimation of source depth) over traditional planewave and range-focused beamforming.

MFP localization performance is limited in practice by high redundancy in the MFP steering vectors, which results in spatial ambiguities in MFP output. These ambiguities, which are often signficant in the range and depth dimensions, can cause large localization errors at low signal-to-noise ratios (SNR's). *Localization* is defined here as estimation of a source location parameter (e.g., source range, depth, or bearing) by maximizing beamformer output over the parameter search space. *Localization error* is defined as the physical distance between the estimated parameter value and the true parameter value, quantified here in a mean-squared sense: $E\left\{\left(\hat{\theta}-\theta_{true}\right)^2\right\}$, where $\hat{\theta}$ is the estimate of the true parameter θ_{true}, and where E is expectation.

For example, consider the MFP range-depth beampattern shown in Fig. 1, for source location 6 km range and 25 m depth. At high SNR's, range/depth estimates for the source will likely fall within the "local error" region surrounding mainlobe of the beampattern. As SNR decreases, however, sidelobe ambiguities become more likley to cause *global errors*, where the source is localized outside the beampattern mainlobe. Several potential global error regions are marked in the Fig. 1.

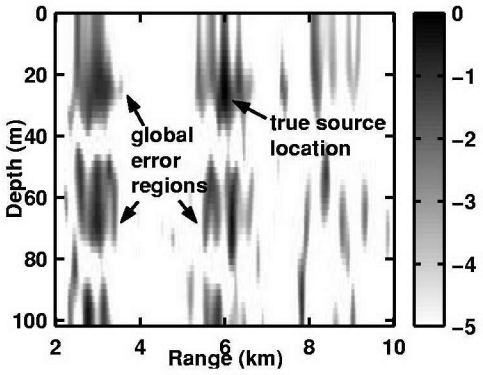

Figure 1: MFP range-depth beampattern for a horizontal line array (length 600 m) at endfire, $\lambda/2$ spacing at frequency 50 Hz. Environment is off the southern California coast. True source location is 6 km range and 25 m depth. Grey scale units are dB (relative to peak).

This work was sponsored by DARPA-ATO under Air Force Contract F19628-00-C-0002. Opnions, interpretations, conclusions, and recommendations are those of the authors and are not necessarily endorsed by the U.S. Government.

Mean-squared error performance curves are typically characterized by three distinct (SNR) "regions" of performance, as depicted in Fig. 2: the *asymptotic region* in which local errors dominate and MSE is proportional to log(SNR); the *threshold region*, in which global errors dominate and MSE rises rapidly as SNR decreases; and the *no information region*, in which the signal is below the noise and location estimates are essentially uniformly distributed. Two important SNR's of interest are the *threshold SNR*, below which global errors become significant, and the *required SNR*, the SNR that is needed to achieve minimum acceptable MSE performance. These SNR's are important for system design, as will be described below. For matched field processing, acceptable performance boundaries often occur within the threshold region, meaning that accurate threshold region performance prediction is vital to understanding what SNR's are truly required for acceptable MFP localization. Ignoring global errors for a local error bound such as

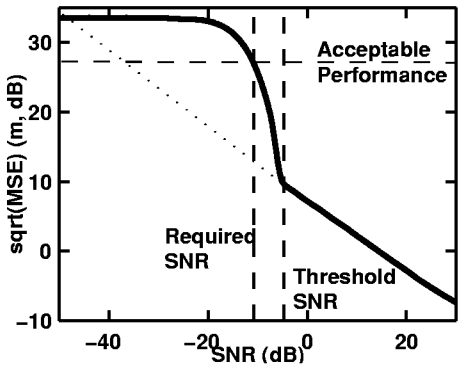

Figure 2: Typical mean-squared error (MSE) performance vs. phone-level SNR. Asymptotic region is all SNR's above -5 dB. Threshold region is between -18 and -5 dB. No information region is below -18 dB.

the Cramér-Rao bound leads to falsely optimistic estimates of the SNR required to achieve acceptable performance. As can be seen in Fig. 2, if the linear part of the MSE curve is extended all the way across the figure, the intersection with the acceptable performance line would occur around -40 dB SNR, much lower than the more accurate estimate of -10 dB required SNR that takes global errors into account.

Clearly, then, quantifying MFP localization performance is a challenging problem. What is needed is accurate *threshold region* MSE performance prediction that takes into account all of the following: ambiguities in the MFP range-depth beampattern (that lead to global errors at low SNR's), signal model mismatch, colored noise, and finite-sample effects (for adaptive beamformers). Previous methods that account for global errors have involved calculating *bounds* which give only approximate performance predictions in the threshold region [2, 7] or have focused on (non-adaptive) maximum likelihood estimation in white noise with known data covariances [1, 8]. The approach taken here is to apply new results [4] to an established technique [5], referred to herein as the *method of interval errors* (MIE), to enable accurate threshold region MFP performance prediction for two popular beamformers in passive sonar, the adaptive Capon-MVDR (CAP) beamformer and the non-adaptive conventional beamformer (CBF). Section 2 describes MIE and the new results that enable its use for CAP and CBF. Section 3 presents some simulation results demonstrating the accuracy of this approach for threshold region performance prediction and also describes a new procedure to extend the MIE framework to include both signal model mismatch and colored noise. Section 4 concludes by summarizing the findings of this work.

2. APPROACH

2.1. Framework

This work assumes a stochastic signal model, as is commonly adopted in passive sonar. Data snapshots $\mathbf{x}$ are assumed to be zero-mean, complex-Gaussian: $\mathbf{x} \sim \mathcal{C}\eta\,(\mathbf{0}, \mathbf{R})$. The covariance $\mathbf{R} = \sigma_s^2 \mathbf{v}_s \mathbf{v}_s^H + \sigma_n^2 \mathbf{R}_n$, where $\mathbf{v}_s$ is the true signal vector, σ_s^2 is the signal power, σ_n^2 is the noise power, and $\mathbf{R}_n$ is the noise covariance, normalized so that its trace equals $|\mathbf{v}_s|^2$ and σ_s^2/σ_n^2 is the phone-level SNR. The sample covariance matrix $\hat{\mathbf{R}}$ is then formed in the usual way: $\hat{\mathbf{R}} = (1/L) \sum_{k=1}^{L} \mathbf{x}_k \mathbf{x}_k^H$, where L is the number of snapshots.

This analysis focuses on estimators that are derived from two popular beamformers in passive sonar, the adaptive Capon-MVDR (CAP) beamformer and the non-adaptive conventional beamformer (CBF). Each estimate is obtained by maximizing the beamformer power output over values of the parameter θ in some search region Θ:

$$\begin{aligned} \hat{\theta}_{\mathrm{CBF}} &= \arg\max_{\theta\in\Theta} \mathrm{CBF}(\theta) \\ &= \arg\max_{\theta\in\Theta} \mathbf{w}_{\mathrm{CBF}(\theta)}^H \hat{\mathbf{R}} \mathbf{w}_{\mathrm{CBF}(\theta)} \qquad (1) \\ \hat{\theta}_{\mathrm{CAP}} &= \arg\max_{\theta\in\Theta} \mathrm{CAP}(\theta) \\ &= \arg\max_{\theta\in\Theta} \mathbf{w}_{\mathrm{CAP}(\theta)}^H \hat{\mathbf{R}} \mathbf{w}_{\mathrm{CAP}(\theta)} \\ &= \arg\max_{\theta\in\Theta} \left(\mathbf{v}_\theta^H \hat{\mathbf{R}}^{-1} \mathbf{v}_\theta \right)^{-1} , \qquad (2) \end{aligned}$$

where the CBF weight vector $\mathbf{w}_{\mathrm{CBF}(\theta)} = \mathbf{v}_\theta / |\mathbf{v}_\theta|^2$ is simply a scaled version of the steering vector $\mathbf{v}_\theta$ at θ and the CAP weight vector is a function of the sample covariance:

$$\mathbf{w}_{\mathrm{CAP}(\theta)} = \hat{\mathbf{R}}^{-1} \mathbf{v}_\theta / \left(\mathbf{v}_\theta^H \hat{\mathbf{R}}^{-1} \mathbf{v}_\theta \right) . \qquad (3)$$

The *maximum likelihood estimate* for the stochastic signal model described above may be derived in the case where

the underlying covariance $\mathbf{R}$ is known but the SNR is unknown. The MLE is given by

$$\hat{\theta}_{\mathrm{MLE}} = \arg\max_{\theta\in\Theta} \left[\mathrm{MF}\left(\theta\right) - \log\left(\mathrm{MF}\left(\theta\right)\right)\right] , \qquad (4)$$

where the *matched filter* output $\mathbf{w}_{\mathrm{MF}(\theta)}^{H}\hat{\mathbf{R}}\mathbf{w}_{\mathrm{MF}(\theta)}$ is a function of the matched filter weight

$$\mathbf{w}_{\mathrm{MF}(\theta)} = \mathbf{R}_n^{-1}\mathbf{v}_\theta / \sqrt{\mathbf{v}_\theta^H \mathbf{R}_n^{-1}\mathbf{v}_\theta} . \qquad (5)$$

Note that (5) depends on knowledge of the underlying noise covariance $\mathbf{R}_n$, which cannot be estimated in passive sonar because signal-free training data is never available. Thus, the MLE serves mainly as a benchmark for MFP performance in this paper. Note, however, that the MLE is equivalent to CBF in the case of white noise ($\mathbf{R}_n = \mathbf{I}$) and known covariance.

2.2. Method of Interval Errors

The **method of interval errors** decomposes the expression for mean-squared error into two conditional probabilities, that an interval error (IE) has occurred or that no interval error (NIE) has occurred, "interval error" being synonymous with "global error" :

$$\begin{aligned} & E\left\{\left(\hat{\theta}-\theta_{true}\right)^2\right\} \\ = \;& Pr\left(\mathrm{NIE}\right) E\left\{\left(\hat{\theta}-\theta_{true}\right)^2 \middle| \mathrm{NIE}\right\} \\ & + Pr\left(\mathrm{IE}\right) E\left\{\left(\hat{\theta}-\theta_{true}\right)^2 \middle| \mathrm{IE}\right\} \\ \approx \;& \left[1 - \sum_{m=0}^{N_m} p\left(\hat{\theta}=\theta_m\right)\right] \times \mathrm{MSE}_{asym} \\ & + \sum_{m=0}^{N_m} p\left(\hat{\theta}=\theta_m\right) \times \left(\theta_m - \theta_{true}\right)^2 , \end{aligned} \qquad (6)$$

where MSE_{asym} represents the asymptotic (high-SNR) MSE and the set $\{\theta_m\}_{m=1}^{N_m}$ represent parameter values corresponding to N_m *sidelobe peaks in the beampattern*. As seen in Eq. (6), MIE approximates the probability of a global error by recognizing that in the threshold region, global errors will almost always occur at sidelobe peaks in the beampattern. This approximation, which turns out to be highly accurate under a wide variety of conditions, turns what would be a continuous integral into a finite sum. A further savings is attained by employing a *union bound* approximation:

$$p\left(\hat{\theta}=\theta_m\right) \approx p_e = p\left(\mathrm{BF}\left(\theta_m\right) > \mathrm{BF}\left(\theta_{true}\right)\right) , \qquad (7)$$

where $\mathrm{BF}\left(\theta\right)$ is the beamformer power at position θ (e.g., $\mathrm{CAP}\left(\theta\right)$ or $\mathrm{CBF}\left(\theta\right)$), and where the right-hand side of (7) is the dominant *pairwise error probability* p_e in the union bound. Substituting (7) into (6) gives the form of MIE used here.

Using MIE thus requires two algorithm-specific quantities: the asymptotic MSE, MSE_{asym}, and the pairwise error probability p_e. The expressions for MSE_{asym} are previously established results. For MLE, MSE_{asym} is given by the familiar Cramér-Rao bound (CRB), which may be computed using the Slepian-Bangs formula and depends on $\mathbf{R}^{-1}$ and the vector partial derivative with respect to parameter θ, $\partial\mathbf{v}_s/\partial\theta$. For CAP and CBF, the expressions for MSE_{asym} can be derived using Taylor series expansions of the beamformer output power about the source location $\theta_{true} = \theta_s$ and are given in works by Vaidyanathan and Buckley (VB) [6] and Hawkes and Nehorai (HN) [3], respectively. Both expressions depend on the data $\mathbf{R}$, the first derivative $\partial\mathbf{v}_s/\partial\theta$, and the second derivative $\partial^2\mathbf{v}_s/\partial\theta^2$, and the VB expression also depends on the third derivative $\partial^3\mathbf{v}_s/\partial\theta^3$. Because MFP steering vectors are superpositions of normal mode functions that are environment-dependent, the vector derivatives cannot be represented analytically and must be computed numerically using finite differences. For the results presented in this paper, it was found that a step size of 0.01 m was sufficient to compute the numerical vector derivatives accurately for both range and depth. (Note that the derivatives need only be computed at the source location.)

The important results that allow application of MIE to both CAP and CBF are the pairwise error probabilities p_e recently derived by Richmond [4] for CAP and CBF. Again, p_e represents the probability that the beamformer power at some location θ_m will exceed that power at the true source location $\theta_{true} = \theta_s$. The procedure for computing p_e for CAP is as follows (the derivation is found in [4]):

1. Define the $N \times 2$ matrix $\mathbf{V} = [\mathbf{v}_m | \mathbf{v}_s]$, where $\mathbf{v}_m$ is the steering vector corrsponding to the sidelobe peak θ_m, then compute the QR-decomposition of $\mathbf{R}^{-1/2}\mathbf{V}$,

$$\mathbf{R}^{-1/2}\mathbf{V} = \mathbf{Q}\begin{bmatrix} \mathbf{D}_{2\times 2} \\ \mathbf{0}_{(N-2)\times 2} \end{bmatrix} ,$$

   and let $\mathbf{d}_1$ and $\mathbf{d}_2$ denote the two 2×1 columns of $\mathbf{D}$.

2. Compute the eigenvalues of the 2×2 matrix $\mathbf{d}_2\mathbf{d}_2^H - \mathbf{d}_1\mathbf{d}_1^H$ and denote the eigenvalues as λ_1 and λ_2.

3. The error probability p_e for CAP is then given by

$$\begin{aligned} p_e \;=\; & 0.5 \cdot \left[1 + \mathrm{sgn}\left(\lambda_1\right)\right] \\ & -\mathrm{sgn}\left(\lambda_1\right) \cdot \mathcal{F}\left(-\lambda_2/\lambda_1, L-N+2\right) , \end{aligned} \qquad (8)$$

   where

$$\mathcal{F}\left(x, N_0\right) \triangleq \frac{x^{N_0}}{\left(1+x\right)^{2N_0-1}} \sum_{k=0}^{N_0-1} \binom{2N_0-1}{k+N_0} \cdot x^k$$

is the cumulative distribution function for a special case of the complex central F statistic.

To compute p_e for CBF, follow the same procedure as above with the following modifications: replace $\mathbf{R}^{-1/2}$ by $\mathbf{R}^{1/2}$ in Step 1, use the 2×2 matrix $\mathbf{d}_1\mathbf{d}_1^H - \mathbf{d}_2\mathbf{d}_2^H$ (instead of $\mathbf{d}_2\mathbf{d}_2^H - \mathbf{d}_1\mathbf{d}_1^H$) to compute the eigenvalues λ_1 and λ_2 in Step 2, and replace $L - N + 2$ by L in Step 3.

3. SIMULATION RESULTS

The simulation results that follow are for a horizontal line array with $N = 41$ elements and 15 m spacing (total aperture 600 m). The array was assumed straight and its depth was assumed to be 100 m. MFP replicas were generated using the KRAKEN normal mode model for an environment near the Santa Barbara channel, with depth 568 m and downward-refracting sound speed profile. Beamformer outputs (from which MFP range and depth estimates were derived) were computed over a search interval of 2-10 km range and 1-101 m depth, at endfire. Beamformer outputs were generated using a sample covariance $\hat{\mathbf{R}}$ with $L = 60$ snapshots ($L \approx 1.5N$).

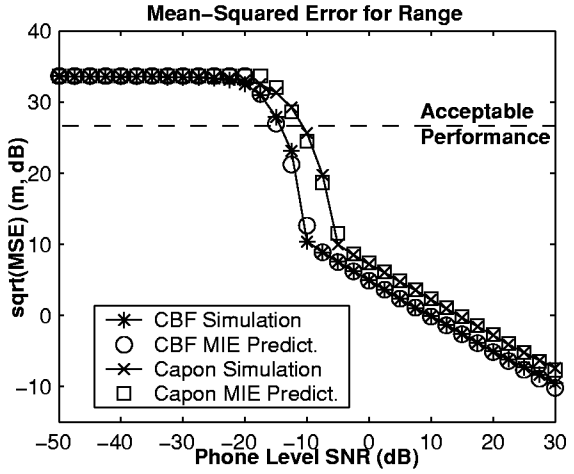

Figure 3: MFP mean-squared error for range estimation versus phone-level SNR for signal in white noise (no mismatch) scenario.

In the first simulation, a 50 Hz endfire source was placed at 6 km range and 25 m depth and the noise was assumed to be white ($\mathbf{R}_n = \mathbf{I}$) and Gaussian with power $\sigma_n^2 = 70$ dB. In the white noise case, parameter estimates derived from CBF and from MLE are identical. Figs. 3 and 4 show the prediction results for estimation of MFP range and depth, respectively.[1] The results compare the MIE predictions of

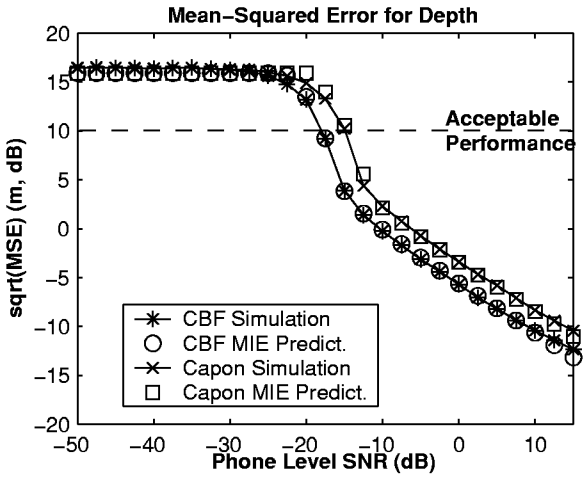

Figure 4: MFP mean-squared error for depth estimation versus SNR for signal in white noise (no mismatch) scenario.

MSE for CBF and CAP (as a function of phone-level SNR) to MSE curves generated from 4000 Monte Carlo runs at each SNR point. MIE predictions for both range and depth and both CBF and CAP are accurate for all SNR's, but most importantly the predictions are accurate within 1-2 dB in the threshold region. Note that in the absence of interferers, CBF/MLE outperforms CAP because CAP suffers losses due to finite-sample adaptive training. Boundaries on acceptable values of $\sqrt{\text{MSE}}$ were taken nominally to be 500 m in range (i.e., significantly better than the mainlobe range resolution of range-focused beamforming at the same frequency, $\approx$ 2.5 km at 2 km range) and 10 m in depth (i.e., enough to enable discrimination of surface and submerged sources). Note again that these boundaries fall well within the threshold region for both range and depth. Thus, predicting the threshold region MSE well is vital to predicting the required phone-level SNR (denoted SNRr here) for acceptable MFP localization. In Fig. 3, SNRr is ≈ -14.5 dB for CBF and ≈ -11 dB for CAP, while in Fig. 4, SNRr is ≈ -17.8 dB for CBF and ≈ -14.8 dB for CAP.

Because MIE predictions are based on the beampattern of a source at a specific location, it is important to understand how performance varies as source location varies. To do this, one may re-compute the curves of Figs. 3 and 4 for each source range and depth in the search space, derive SNRr for both range and depth, and use the higher of the two SNRr values as the overall SNRr at a given source location. For CBF in the current scenario, this procedure reveals a 3-5 dB variation in SNRr over the range-depth search space. From the values of SNRr, one can back out the source levels required for acceptable MFP localization by adding back

[1] In this paper, range and depth were estimated separately, with the other parameter assumed known. MIE has a straightforward extension to simultaneous estimation of range and depth, but simulating the latter is much more time-consuming.

the noise level of 70 dB and the predicted transmission loss (TL) at each source location.[2] This computation is shown in Fig. 5 for CBF. Note that the source levels shown in Fig. 5 are reflective of the ideal nature of this scenario, white noise and no mismatch.

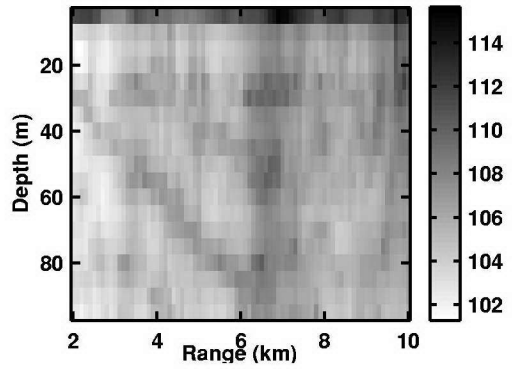

Figure 5: Required source levels for acceptable MFP localization using CBF, as function of source range and depth. Gray scale units are dB re: 1 μPa/Hz.

When signal model **mismatch** is introduced into the problem, the MIE procedure needs to be modified to account for the possibility that $\hat{\theta}$ may never converge even asymptotically (with increasing SNR) to θ_{true} [4]. Most often, $\hat{\theta}$ will converge to some *mismatched* value θ_{MM} and there will be an asymptotic bias in MSE equal to $|\theta_{true} - \theta_{MM}|^2$. To account for this, one needs to compute MSE_{asym} using the true data $\mathbf{R}$ and the *mismatched* vector $\mathbf{v}_{MM}$ (corresponding to location θ_{MM}). Further, the necessary error probabilities p_e describing the transition to the threshold region are now derived from the competition of the local sidelobe peaks of the "mismatched beampattern" (computed by taking normalized inner products of the mismatched steering vector with the true source vector) with the peak mismatched vector $\mathbf{v}_{MM}$.

Thus, the modified MIE expression for MSE is given by (6) and (7), except with θ_{MM} replacing θ_{true} in the pairwise error probabilities and with MSE_{asym} computed using $\mathbf{v}_{MM}$ instead of the true source vector $\mathbf{v}_s$. The interval error is still computed relative to θ_{true} in order to reflect the actual accounting of MSE. And the error probabilities are still computed using the procedure detailed in the previous section, with $\mathbf{v}_{MM}$ replacing $\mathbf{v}_s$ in Step 1.

In the second simulation, a mismatch in compressional sound speed of 10 m/s was introduced into the propagation model (true value was 1572, mismatched value was 1562); for this case, the noise was still white. Fig. 6 shows the prediction results for estimation of MFP range in the mismatched case (depth estimation performance was very similar). Note that the mismatch causes a slight degradation in performance in the threshold region and an asymptotic bias of $\approx$ 4 m (5 dB). Importantly, however, the threshold

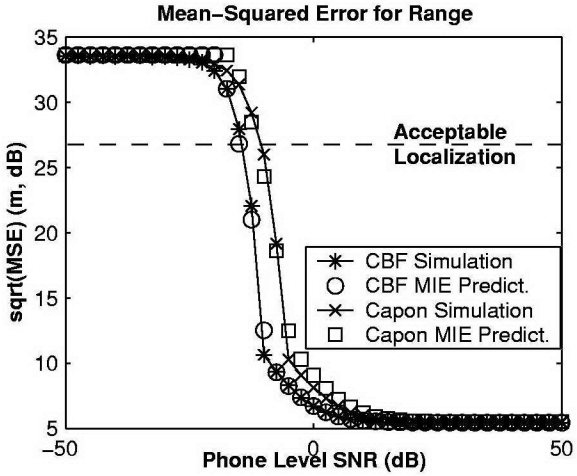

Figure 6: MFP mean-squared error for range estimatiion versus SNR for *mismatched* signal in white noise scenario (mismatch of 10 m/s in compressional sound speed).

region predictions are still accurate within 1-2 dB for both CBF and CAP. Because this scenario again involved white noise, CBF still outperformed CAP because of the adaptive training losses incurred by CAP.

Finally, one can apply the modified MIE procedure for the mismatch case to the **colored noise** (discrete interferer) scenario, for cases where $\mathbf{R}_n$ is fixed (but not white) and where all discrete interferers are located outside the search region.[3] In the specific problem examined here, $\mathbf{R}_n = \sigma_d^2 \mathbf{d}\mathbf{d}^H + \sigma_n^2 \mathbf{I}$, where $\mathbf{d}$ represents the steering vector of a distant interferer and where the interferer power σ_d^2 is held constant while the signal power σ_s^2 (and thus the signal-to-ambient-noise ratio [SANR]) varies. Constant power for distant inteferers is not unusual for passive sonar data, so this is a case of interest.

In this colored noise case, MSE performance for very high SANR's will mirror the asymptotic region of the white noise case, because the signal is dominant and parameter estimates will be near the signal location. As the signal power σ_s^2 (and thus the SANR) decreases, the signal-to-interference ratio σ_s^2/σ_d^2 will decrease and the interferer will become more influential, with increasing likelihood that parameter estimates will be near the largest sidelobe of the interferer within the search space (recall that the interferer itself, $\mathbf{d}$, is located outside the search space). Denote the

[2]The MFP propagation model gives TL for each phone in the array, and one can use the root-mean-squared of all the phone TL's to derive an overall "array TL" at a given source location.

[3]If interferers are located *within* the search region, then the problem becomes a *multi-source* parameter estimation problem. MIE with slight modification still produces accurate performance predictions in this case, as detailed in [4].

steering vector associated with this largest interferer sidelobe as $\mathbf{v}_d$. Then the analogous threshold region MSE performance can be derived by following the same procedure as in the mismatch case outlined above, with $\mathbf{v}_d$ replacing $\mathbf{v}_{MM}$. The added complication here is that the SANR dependence of the "colored beampattern" (computed by taking normalized output of the beamformer weights with the data, both computed using ideal covariances) needs to be accounted for.

For the third scenario, an interferer was introduced at 20 km range, 5 m depth, and 10° bearing, with power $\sigma_d^2 = 66.8$ dB (corresponding to 150 dB source level). Fig. 7 shows the prediction results for estimation of MFP range in the colored case (depth estimation performance was very similar). Note that with the introduction of the interferer, CBF is no longer equivalent to MLE, and CBF performance is degraded significantly, by about 10 dB SNR relative to the white noise case. CBF still outperforms CAP in the asymptotic region (where behavior is like the white noise case), but the adaptive CAP now outperforms CBF in the threshold region, where adaptive interference rejection becomes more beneficial. Note that threshold region performance for

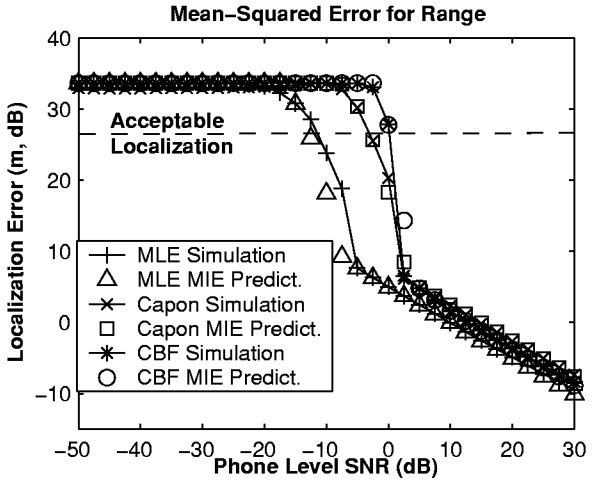

Figure 7: MFP mean-squared error for range estimatiion versus SNR for signal in *colored* noise scenario.

CAP is still well-predicted by MIE within 1-2 dB, while CBF threshold region prediction is off by slightly more because significant interference sidelobes cause greater departures from MIE assumptions.[4]

4. SUMMARY AND DISCUSSION

This work demonstrates a powerful prediction tool for MFP localization performance. Mean-squared error (MSE) prediction was shown to be accurate within 1-2 dB in the threshold region for both MFP range and depth and for both the CBF and Capon-MVDR (CAP) beamformers. Accurate threshold region predictions in turn lead to better estimates of the SNR's (and, equivalently, the source levels) required for acceptable MFP localization. These accurate threshold region predictions for both CBF and CAP were made possible by application of new pairwise error probability results to the established method of interval errors (MIE) technique. Slight modification of the basic MIE procedure also enables accurate threshold region prediction in the cases of signal model mismatch and colored noise, as was demonstrated in separate simulation examples.

It is important to note that because MIE is *situation-specific* (for example, one needs to hypothesize a mismatch mechanism for the signal model mismatch case), definitive quantification of MFP localization performance will require systematic analysis repeating the above simulations over several reasonable mismatch and interference scenarios. Future work may also extend the techniques presented here to the case where sources are moving during the observation interval.

[4]Threshold region performance for MLE is also approximate because precises error probabilities were not computed.

5. REFERENCES

[1] F. Athley. *Space time parameter estimation in radar array processing*. PhD thesis, Chalmers University of Technology, June 2003.

[2] K. Bell et al. Extended Ziv-Zakai lower bound for vector parameter estimation. *IEEE Trans. on Information Theory*, 43(2):624–637, March 1997.

[3] M. Hawkes and A. Nehorai. Acoustic vector-sensor beamforming and Capon direction estimation. *IEEE Trans. on Signal Processing*, 46(9):2291–2304, September 1998.

[4] C. Richmond. Capon algorithm mean squared error threshold SNR prediction and probability of resolution. *IEEE Trans. on Signal Processing*. To appear, 2004.

[5] H. L. Van Trees. *Detection, Estimation, and Modulation Theory Pt. I*, pages 278–286. Wiley, NY, 1968.

[6] C. Vaidyanathan and K. Buckley. Performance analysis of the MVDR spatial spectral estimator. *IEEE Trans. on Signal Processing*, 43(6):1427–1437, June 1995.

[7] W. Xu. *Performance bounds on matched-field methods for source localization and estimation of ocean environmental parameters*. PhD thesis, MIT, June 2001.

[8] W. Xu, A. Baggeroer, and H. Schmidt. Quantitative ambiguity analysis for matched-field source localization. In *Proc. 36th Asilomar Conf.*, pages 448–452, 2002.

ATO

Threshold Region Performance Prediction for Adaptive Matched Field Localization

Nigel Lee and Christ D. Richmond

MIT Lincoln Laboratory

Adaptive Sensor and Array Processing Workshop

16 March 2004

This work was sponsored by DARPA/ATO under Air Force contract F19628-00-C-0002. Opinions, interpretations, conclusions, and recommendations are those of the authors and are not necessarily endorsed by the U.S. Government.

The MFP Localization Problem

Shallow-Water Multipath Propagation:

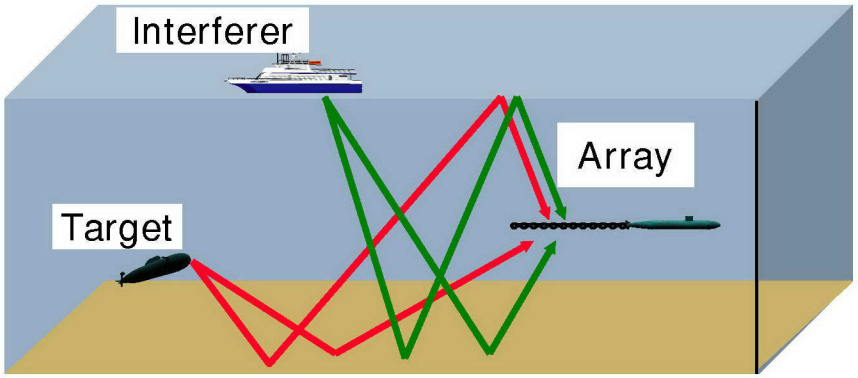

Matched field processing (MFP)
models acoustic multipath propagation
to enable 3-D source localization

- Goal: quantify what SNR's are required for acceptable MFP localization
- Approach: accurate MFP mean-squared error prediction that accounts for
  - Ambiguities in MFP output
  - Signal model mismatch
  - Colored noise (discrete interferers)
  - Adaptive training effects
- Challenge: previously no way to achieve above for specific adaptive beamformers

MFP Beampattern for Vertical Array
(good aperture for MFP)

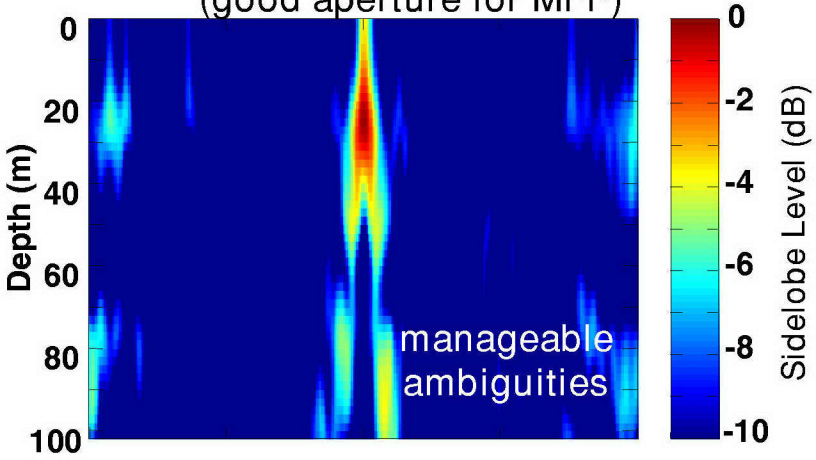

MFP Beampattern for Horizontal Array, Endfire
(poor aperture for MFP)

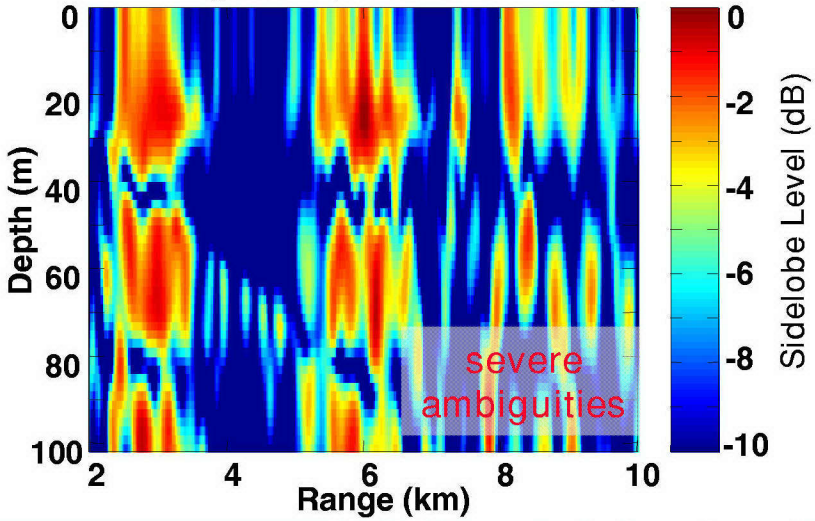

Mean-Squared Error (MSE) Performance Prediction

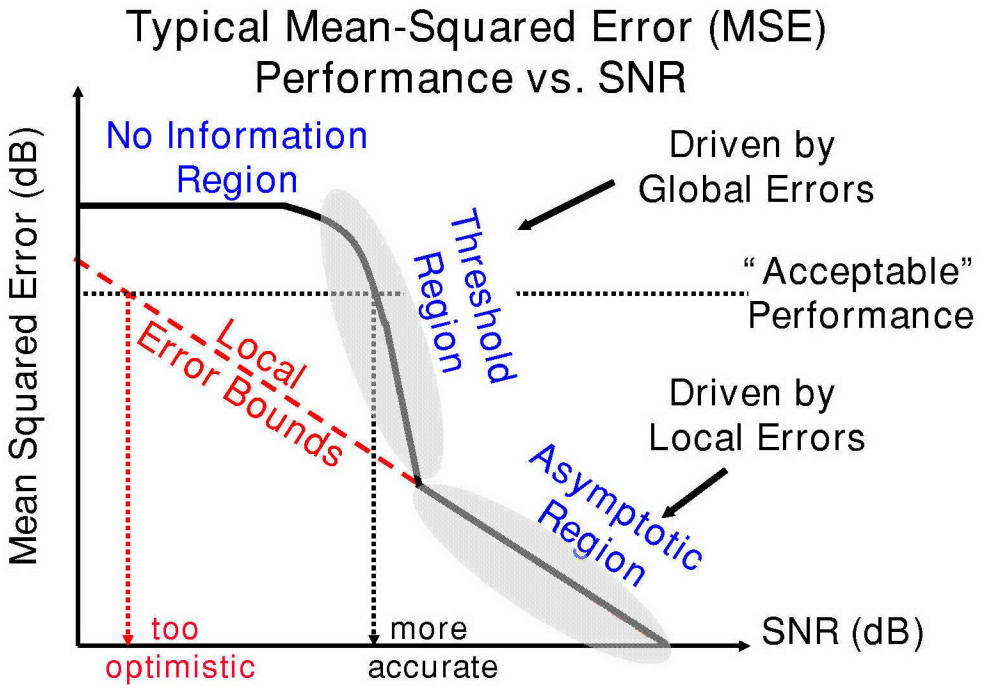

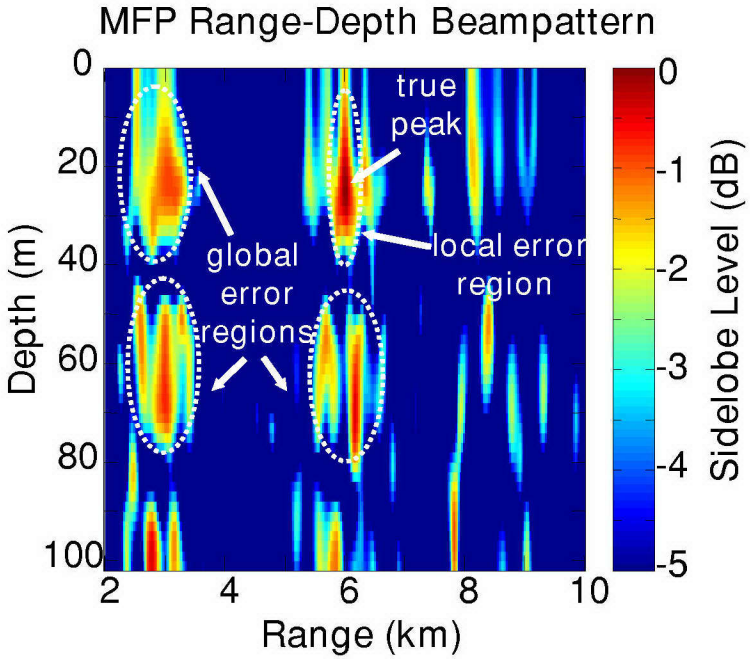

- Boundary for acceptable MFP performance often occurs in threshold region ⇒ must predict threshold region accurately

- How?

Beamformers:
Capon-MVDR (adaptive)
CBF (non-adaptive)